Timaru District Coastal Hazard Assessment

Coastal Inundation

Prepared for Environment Canterbury

June 2020

Prepared by:
Cyprien Bosserelle
Jade Arnold

For any information regarding this report please contact:
Cyprien Bosserelle
National Institute of Water & Atmospheric Research Ltd
10 Kyle Street, Riccarton, Christchurch 8011

PO Box 8602, Christchurch

Phone +64 3 341 2040

NIWA CLIENT REPORT No: 2020072HN
Report date: June 2020
NIWA Project: JEI20201

Quality Assurance Statement		
	Reviewed by:	Richard Measures
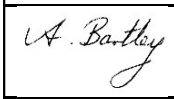	Formatting checked by:	Alison Bartley
	Approved for release by:	Scott Stephens

© All rights reserved. This publication may not be reproduced or copied in any form without the permission of the copyright owner(s). Such permission is only to be given in accordance with the terms of the client's contract with NIWA. This copyright extends to all forms of copying and any storage of material in any kind of information retrieval system.

Whilst NIWA has used all reasonable endeavours to ensure that the information contained in this document is accurate, NIWA does not give any express or implied warranty as to the completeness of the information contained herein, or that it will be suitable for any purpose(s) other than those specifically contemplated during the Project or agreed by NIWA and the Client.

Contents

Tables

Figures

Executive summary

Environment Canterbury (ECan) and the Timaru District Council (TDC), require a coastal hazard assessment for the Timaru District coastline. Jacobs New Zealand Ltd (Jacobs) and the National Institute of Water and Atmosphere (NIWA) have been contracted to provide ECan and TDC a coastal hazard assessment of the Timaru District coastline with the NIWA team focussing on the coastal inundation hazard and the Jacobs team focussing on the coastal erosion hazards. This report describes the coastal inundation hazard assessment and the inundation hazard zones which have been generated. The assessment uses nine scenarios in total; the present-day 1% annual exceedance probability (AEP) storm combined with sea-level rise (SLR) increments of 0, 0.2, 0.4, 0.6, 0.8, 1.2 and 1.5 m, and a 2% AEP storm with 0.4 and 0.6 m SLR. This approach is consistent with Coastal hazards and climate change guidance for local government (MfE, 2017) for testing adaptation plans against a range of SLR increments.

This assessment makes use of the process-based model XBeach_GPU to simulate inundation due to the combined contributions of extreme storm-tide and waves previously reported in the ECAN Coastal Hazard Calculator (Stephens et al. 2015). GIS layers accompanying this document show the details of flow depth and maximum water-level. The 1% AEP simulation at present-day mean sea-level produces significant inundation throughout the district generally consistent with the existing Sea Water Inundation Boundary (ECAN). Simulation including incremental SLR shows increasing inundation. The inundated area for the 1% AEP doubles with 0.8 m SLR; for 1.5m SLR the area increases 2.5 times.

Between Washdyke Lagoon and the Rangitata River there are stop-banks present along the coast. Although overtopped during large coastal storms, these are effective at limiting the inundation extent, but the effect of these structures diminishes with SLR. The role of stop-banks is important in monitoring and planning for climate change adaption pathways. In South Timaru, the inundation extent can exceed the area covered by LiDAR topography leading to uncertainty in the results there.

The study has limitations inherent to the scenarios and the methodology. Validation simulations of historical storms showed model results consistent with observations, although the comparison does show a slight tendency for the model to underestimate inundation. However, the overall approach is conservative as the design scenarios are based on an upper bound estimate of the 2% and 1% AEP wave conditions. As such the computed inundation extents/water levels should not require the inclusion any additional safety factor (i.e., freeboard) to the presented inundation layers.

1 Introduction

Environment Canterbury (ECan) and the Timaru District Council (TDC), require a coastal hazard assessment along the Timaru District coastline. Jacobs New Zealand Ltd (Jacobs) and the National Institute of Water and Atmosphere (NIWA) have been contracted to provide ECan and TDC a coastal hazard assessment of the Timaru District coastline with the NIWA team focussing on the coastal inundation hazard and the team from Jacobs focussing on the coastal erosion hazards. This report presents findings on the coastal inundation hazard assessment as well as mapped inundation hazard overlays. The assessment uses nine scenarios for different Averaged Recurrence Interval (ARI) (or corresponding Annual Exceedance Probability (AEP)) (Table 1-1) including sea-level rise (SLR) scenarios out to the year 2130 (see section 2.5.1). This approach is consistent with the recommended guidance for testing adaptation plans against a range of SLR increments (MfE 2017) and with the NZCPS directive to avoid coastal hazard risk over at least the next 100 years (DoC, 2010).

The scope of the study is to produce inundation maps for the Timaru district between the Rangitata River in the North and the Pareora River in the South (Figure 1-1). This assessment makes use of the process-based model XBeach_GPU to simulate inundation due to the combined contribution of extreme storm-tide and waves previously calculated by Stephens et al. (2015). River inundation is outside the scope of this study but realistic flow (mean annual-maximum river flow) is included in the model for the Orari, Opihi, Rangitata and Pareora rivers. Other sources of inundation (tsunami, groundwater inundation) are not considered here.

Table 1-1: Coastal Inundation output scenarios. See section 2.5.1 for details on the scenarios.

Likelihood	SLR scenario relative to present-day mean sea level (m MSL)
1% AEP (100-year ARI)	0.0, 0.2, 0.4, 0.6, 0.8, 1.2, 1.5
2% AEP (50-year ARI)	0.4, 0.6

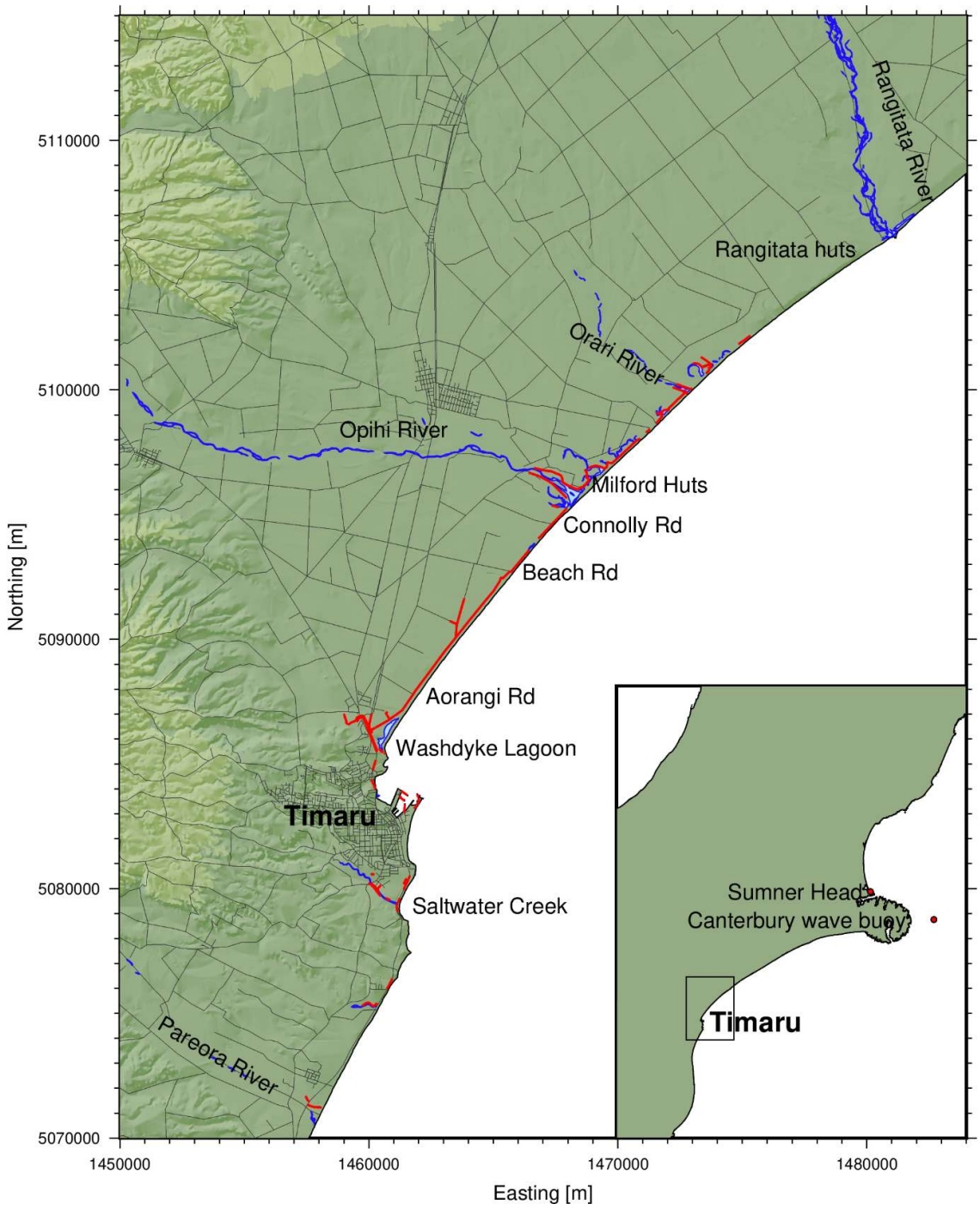

Figure 1-1: Timaru coastline location map. Note: red lines show digitised flow structures (e.g., stopbanks road embankment, seawall).

1.1 Accompanying files

Results from the nine coastal inundation scenarios (Table 1-1) are mapped as inundation hazard overlays, setting the coastal hazard context along the Timaru District Coast. The results are presented in accompanying GIS layers containing maximum water level, depth and extent for each inundation scenario (file naming conventions described in Table 1-2). The report text and figures provide a detailed description of the methodology and an overview of the results.

Table 1-2: Description of files accompanying the study. Files are provided for each separate scenario where all model grids have been collated. Scenario details can be found in section 2.5.

File name	Type (resolution)	Description
ScenarioARI_Maximum-Water-Level_***SLR***.tif	GeoTiff Raster (10 m)	Maximum water level for inundation model in GeoTiff format. ***ScenarioARI*** is either *50-yearARI* or *100-yearARI*. ***SLR*** is the value as shown in Table 1-1.
ScenarioARI_flowDepth_***SLR***.nc	GeoTiff Raster (10 m)	Maximum water depth for inundation model in GeoTiff format. ***ScenarioARI*** is either *50-yearARI* or *100-yearARI*. ***SLR*** is the value as shown in Table 1-1.
ScenarioARI_InundationContour_***SLR***.shp	polygon (shapefile)	Maximum inundation extent line in shapefile format. ***ScenarioARI*** is either *50-yearARI* or *100-yearARI*. ***SLR*** is the value as shown in Table 1-1.

2 Methodology

The scope of the study is to simulate and map the impacts of the nine coastal-inundation scenarios (Table 1-1) using a process-based two-dimensional model forced with storm-tide and wave boundary conditions derived from previous calculations reported in Stephens et al. (2015).

2.1 Model description

The process-based model XBeach_GPU (Bosserelle, 2013) which is a variant of XBeach (Roelvink et al. 2009) is used for the inundation simulations. XBeach_GPU uses the same wave-group resolving wave model and coupled hydrodynamics model as XBeach but the models are optimised to run on Graphics Processing Units (GPU or graphics cards) for improved computational speeds. XBeach_GPU has been validated against XBeach for identical model domain and inputs[1]. The model explicitly includes waves, simulated as group-varying wave energy, and storm-tide simulated in a shock-capturing hydrodynamics model tightly coupled to the wave model. The coupled model allows the simulation to explicitly account for wave transformations in the nearshore, and the interaction between waves, currents and water levels in the surf zone. The simulation of surf-zone dynamics is important for inundation simulations because it takes into account infragravity wave generation, propagation and dissipation. Maximum inundation is calculated on the two-dimensional grids as the maximum water level and maximum flow depth over the duration of the simulation (3 h).

River inundation is outside the scope of this study but realistic flow (mean annual-maximum river flow) is included in the model for the Orari, Opihi, Rangitata and Pareora rivers. The model is setup on a topographic grid at 10 m resolution accounting for variation in beach slope cross-shore and alongshore.

2.2 Bathymetry/ Topography

Model accuracy is highly dependent on the accuracy of the topography and bathymetry of the model. Therefore, extra care needs to be taken in preparing the model grids.

2.2.1 Datum

All maps presented in this report (and accompanying files) are in New Zealand Transverse Mercator 2000 (EPSG:2193) projection (hereafter NZTM2000) and all elevation data used in the model and results are relative to the Lyttelton Vertical Datum 1937 (hereafter LVD). Relationship between LVD and other vertical datums is given in Table 2-1.

Table 2-1: Relationship between LVD and other vertical datums.

Vertical datum	Height relative to LVD [m]
New Zealand Vertical Datum 2016 (NZVD16)[2]	0.33 – 0.39
Mean Sea Level (MSL) (period between 1993 and 2012)	0.17
Chart Datum (CD)	-1.27
Port Timaru tide gauge zero	-1.30

[1] See https://github.com/CyprienBosserelle/xbeach_gpu/wiki/Validation

[2] See LINZ data service: https://data.linz.govt.nz/layer/53432-lyttelton-1937-to-nzvd2016-conversion/

2.2.2 Data sources

Bathymetry and topography datasets were collated from various sources. These were offset to LVD where necessary. Collated data was then combined, prioritising the LiDAR and survey datasets, and using other datasets to fill-in any gaps. The resulting consolidated dataset was then rotated to each grid coordinate system (See Section 2.2.3 below) and interpolated onto a uniform grid using a continuous spline in tension (Smith and Wessel 1990). In locations where significant gaps existed between bathymetric survey and LiDAR coverage, a visual interpretation of satellite imagery was used to create contours to help constrain the interpolation between datasets (see section 2.2.4 for more details).

Table 2-2: Bathymetry-Topography data sources.

Bathymetry/topography data source	Original Vertical Datum	Provider/Comment
LiDAR: NZAM 10027 Timaru Town and Coast (2010)	LVD	Environment Canterbury
LiDAR: FPFA1073 Timaru Rivers (2014)	LVD	Environment Canterbury
Bathymetry contour and soundings	Chart Datum	LINZ
Caroline Bay bathymetry survey	Chart Datum	Environment Canterbury
15 m topomap derived DEM (Columbus 2011)	MSL (date unclear)	University of Otago

2.2.3 Model grid layout

XBeach_GPU requires the model grid to lay roughly parallel to the coast with the left boundary directly offshore (where the wave energy is applied). The coast of the district of Timaru was divided into four grids (Figure 2-1) at 10 m resolution with a small overlap between the grids.

Available LiDAR, soundings and survey data were adjusted to the LVD datum where necessary. For each grid the datasets were rotated to that grid's coordinate system and interpolated onto the 10 m grid.

After running the models, results from the four model grids were rotated back to a single 10 m NZTM2000 grid covering the district. Where two grids overlapped the maximum value of inundation was selected for NZTM2000 grid.

All the results presented in this report and in accompanying GIS files are relative to the NZTM2000 coordinate system.

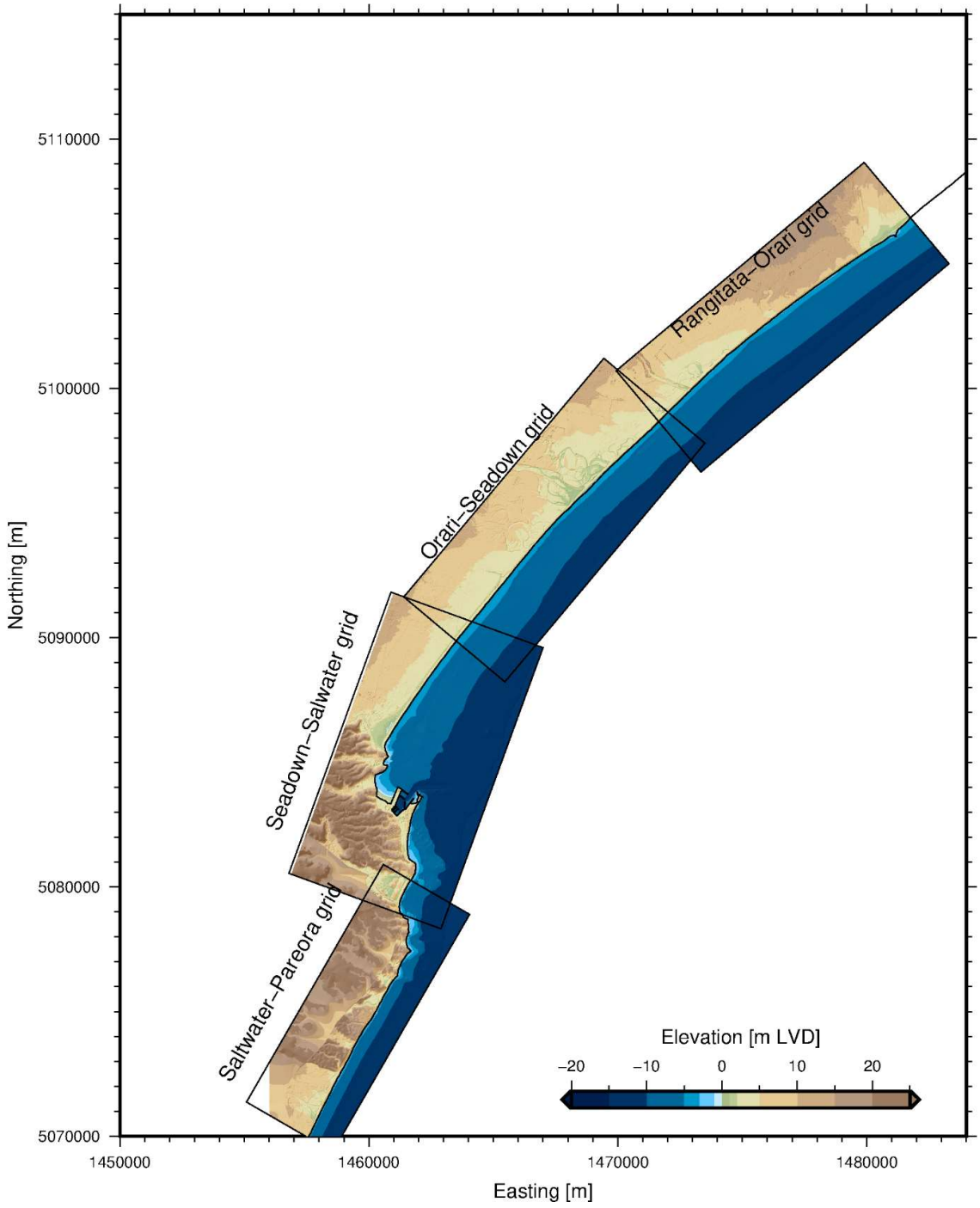

Figure 2-1: Model grids layout for Timaru district. Note: LiDAR data is not available for the backshore between Saltwater Creek and Pareora. The DEM derived from topomaps has been used there instead.

2.2.4 Manual bathymetry enhancement

Some manual bathymetry/topography enhancements were necessary to compensate for missing data and up-sampling artefacts.

Soundings and bathymetry contours north of Timaru do not cover the nearshore area. To use a simple interpolation would miss out the beach step leading to an unrealistically shallow nearshore area. In order to include a beach step and force the interpolation to maintain a realistic profile in the bathymetry of the nearshore we placed a contour along the offshore edge of the surf-zone at -2.9 m LVD (equal to 1.64 m CD or approximately 3.0 m below MSL). This value is consistent with the surveyed beach step at Washdyke Lagoon (Cope and Young 2001).

Reducing LiDAR topography from 1m resolution to a 10 m grid can lead to incorrect averaging of the elevation of narrow features (those narrower than the model resolution) such as narrow drains and narrow stopbanks. In order to correctly assess the role of the stopbanks and drains the narrow features in the model grid were enhanced to match the height in the original LiDAR. First, narrow stopbanks and drains were digitized (see Figure 1-1) using the 1 m LiDAR then all the cells in the interpolated grids within a critical distance of the digitized feature (taken as the feature width) would automatically be assigned the elevation of the digitized feature. While this task is time consuming it is critical to accurately simulate the effects of stopbanks and drains on inundation.

2.3 Bed roughness

Land use and vegetation roughness play an important role in controlling inundation by slowing the propagation of flood water and thus limiting the inundation extent (e.g., Zhang et al. 2012). Here the categorising technique from Townsend and Wadhwa (2017) was used to define different vegetation and land use types, and to map on-land roughness. XBeach_GPU was set up with variable roughness with friction coefficients compatible with the XBeach Chezy formulation (Table 2-3 and Figure 2-2).

Following a similar process as with the bathymetry, the roughness information was rotated and interpolated onto the model grids. The roughness grids have identical layouts as the bathymetry grids.

Table 2-3: Summary of friction coefficient based on Chezy values for various land use classification.

Vegetation land use classification	dimensionless friction coefficient (cf)	Reference/source
Muds	0.015	(Chow 1959)
Sands	0.026–0.035 (used range relative to depth)	(Chow 1959; Arcement & Schneider 1989)
Mangroves	0.01–0.22 (0.1 used)	(Musleh & Cruise 2006)
Wetlands	0.04–0.1 (0.04 used)	(Narayan et al. 2017)
Kiwifruit Orchards	0.025–0.12 (used 0.05) estimated low vegetation density	(Arcement & Schneider 1989)
Exotic forest	0.085–0.120 (0.11 used)	(Arcement & Schneider 1989)
Grass (Meadow?)	0.01–0.08 (0.02 used)	(Henderson 1966; Engman Edwin 1986; Arcement & Schneider 1989)
Buildings	1	-
Roads	0.012–0.016 (0.013 used)	(Ali 2001)
Lakes/water bodies	0.01	(Narayan et al. 2017)

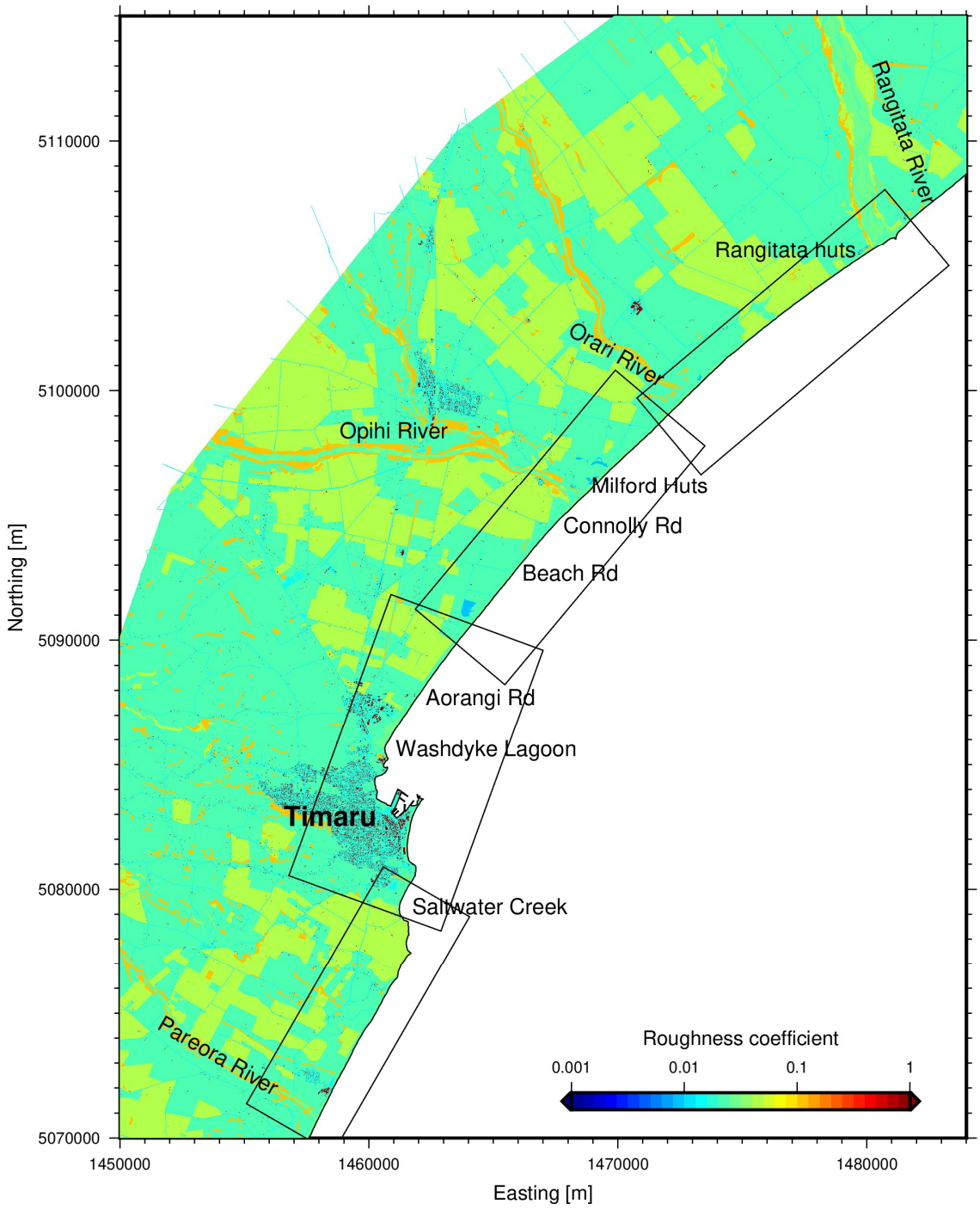

Figure 2-2: On land roughness map used in model simulations. Seabed roughness for the coastal area (not mapped here) was considered constant at 0.01.

2.4 Model parameters

XBeach_GPU consists of a wave model and a hydrodynamics model that interact at every computational step. Each model has parametrisations to account for processes not explicitly simulated or that occur at a smaller scale than the model resolves (e.g., wave breaking, turbulence). The simulations use most of the default standard model parameters (see Table 2-4) based on studies of dissipative beaches in East Coast US and Northern Europe (Deltares 2019). However, calibration of the model on historical storm inundation suggests that a higher wave breaking intensity parameter (gamma) is more suitable (See Section 2.6).

Table 2-4: XBeach_GPU model parameters. More detail about the parameters can be found in the XBeach manual available at https://xbeach.readthedocs.io/.

Parameter name (XBeach name in manual)	Description	Value
Drying height (ε)	Minimum water depth for water to flow	0.02 m
Current friction (cf)	Chezy bottom friction parameter (See Section 2.3)	Variable
CFL	CFL limiter for calculating time step	0.6
Smagorinsky coefficient	Coefficient for Smagorinsky formulation of eddy viscosity	0.3
Minimum wave direction (θ_{min})	Minimum wave direction relative to the model X axis positive clockwise	-60°
Maximum wave direction (θ_{max})	Maximum wave direction relative to the model X axis positive clockwise	60°
Directional bin width in wave model (d_θ)	Direction bin width in wave model	10°
Wave friction (f_w)	Wave bottom dissipation	0.001
Wave breaking dissipation ($gamma$)	Breaker index	0.75
n parameter in Roelvink wave dissipation	Breaker shape factor	10
Wave roller dissipation ($beta$)	Breaker slope coefficient in roller model	0.1

2.5 Model forcing

The model was forced along the offshore boundary with storm-tide and wave spectral information (used to calculate wave group energy and long-bound waves). The water level at the coast resulting from the interaction between storm-tide, wave setup and infragravity waves is calculated by the model.

The sea-level elevation on the grid boundary is raised from 1.2 m LVD to the storm-tide level over the first 60 minutes of simulation and then kept constant for the rest of the simulation (2 hours). The wave spectral forcing was assumed constant for the entire duration (3 hours). The spectral information was forced with significant wave height (Hs) (varies between grids and scenarios), peak wave period (Tp) (15.5 s assumed for all scenarios based on historical storms, see Table 2-9) and peak

direction (Dp) (assumed normal to the offshore boundary of each grid for all scenarios). A JONSWAP spectral shape was assumed to estimate the wave energy-frequency distribution. Although the wave spectral forcing is constant, the model automatically incorporates wave groups and associated long-bound waves. Wave groups and long-bound waves are automatically calculated at the model boundary at the start of each 3-hour simulation.

While most storms persist for longer than 3hrs, analysed historical storm peaks generally persisted for less than 6 hrs and inundation historically occurred when the storm peak coincided with high-tide (Section 2.6).

Each of the four separate grids representing the different parts of Timaru District use slightly different forcings based on the estimated wave and storm tide conditions from Stephens et al. (2015). The simulation was forced with values of wave height of the 95th percentile confidence interval. This forcing is conservative compared with forcing with maximum likelihood significant wave height but removes the need for including any additional safety factor (i.e., freeboard) to the model final results.

Storm-tide and wave parameters are given in Table 2-5 for the 1% AEP (1% AEP) and in Table 2-6 for the 2% AEP (2% AEP). The storm-tide and wave forcing parameters in Table 2-5 were derived from the Coastal Calculator, which was validated against historical storm runup observations (Stephens et al. 2015). Storm tide elevations are consistent across the district but wave conditions area greater in the southern part of Timaru district.

Table 2-5: Model forcing for the 1% AEP (100-year ARI) storm conditions. Note: Maximum likelihood Hs is given as an indication. The 95th percentile confidence interval Hs was used in the simulations.

Grid	Corresponding profile in Stephens et al. 2015	Storm tide (m LVD) 1% AEP	Significant wave height (Hs) (m) 1% AEP maximum Likelihood	Significant wave height (Hs) (m) 1% AEP 95th percentile
Rangitata Orari	Rangitata river mouth	1.78	5.07	6.93
Orari to Seadown	Washdyke North	1.78	5.14	6.99
Seadown to Saltwater	Timaru South Beach	1.78	5.36	7.46
Saltwater Pareora	Craigie Road	1.78	5.57	7.8

Table 2-6: Model forcing for the 2% AEP (50-year ARI) storm conditions. Note: Maximum likelihood Hs is given as an indication. The 95th percentile confidence interval Hs was used in the simulations.

Model grid	Corresponding profile in Stephens et al. 2015	Storm tide (m LVD) 2% AEP	Hs 2% AEP max Likelihood (m)	Hs 2% AEP 95th percentile (m)
Rangitata Orari	Rangitata river mouth	1.75	4.75	6.28
Orari to Seadown	Washdyke North	1.75	4.82	6.35
Seadown to Saltwater	Timaru South Beach	1.75	4.95	6.66
Saltwater Pareora	Craigie Road	1.75	5.18	7.01

2.5.1 Sea-level rise

The SLR scenarios in Table 1-1 are consistent with the range of SLR scenarios to the year 2070 and 2130 in Table 10 of MfE (2017) (Table 2-7 below). The upper three SLR scenarios of 0.8 m, 1.2m and 1.5 m correlate to the RCP 4.5 median, RCP 8.5 median and RCP8.5 H+ (83rd percentile) projections respectively for a 2130 timeframe. This is also consistent with Policies 24 and 25 of the NZCPS to identify and avoid coastal hazard risk over at least the next 100 years (DoC 2010). The use of other scenarios of 0.2, 0.4 and 0.6 m, covers the range of projections for the next 50 years to 2070, and is consistent with the recommended guidance to test adaptation plans against a range of SLR increments (MfE 2017).

Table 2-7: SLR projections (metres above 1986–2005 baseline MSL) in 2070 and 2130 for the wider New Zealand region.

Year	NZ RCP2.6 M (median)	NZ RCP4.5 M (median)	NZ RCP8.5 M (median)	NZ RCP8.5 H^+ (83^{rd} percentile)
1986–2005	0	0	0	0
2070	0.32	0.36	0.45	0.61
2130	0.60	0.74	1.18	1.52

2.5.2 River Flow

River flooding is not considered in this study. However, river flow was incorporated into the model as a constant flux boundary in the river bed on the landward extent of the model for the Rangitata River, Opihi River, Orari River and Pareora River. Simulating rivers with only averaged flow was not considered suitable since coastal inundation can coincide with high rainfall and/or river flooding. On the other hand, simulating coastal inundation with extreme river flow was also considered to be unrealistic since the 100-year coastal inundation is not likely to coincide with the 100-year river flood. In a compromise between these two extreme situations and in the absence of robust joint-probability analysis, it was decided to simulate the flow with a mean annual-maximum flow for each of the main rivers, based on the downstream most reliable flow recorder data (Table 2-8).

Table 2-8: River flows used in simulations.

River	mean annual-maximum flow (m^3/s)	Period of record used to calculate mean (only considering years with >90% record)
Opihi (at SH1 Bridge)	344	1999-2019
Orari (at Ohapi Ck confluence)	219	2007-2019
Temuka (at Manse Br)	299	1992-2019
Pareora (at SH1)	387	2009-2019
Rangitata (at Klondyke)	1145	1980-2019

2.6 Calibration and validation

The coastal storm of 20 July 2001 reported by Cope and Young 2001 was used to calibrate the breaker index (*gamma*) parameter. The model was tested for the entire valid range of the parameter (0.5 to 0.8 at a 0.05 interval) while other parameters remained constant. Several other storms were used to verify simulated wave runup using evidence from inundation photos of runup. These storms were selected because they were mostly a coastal inundation event and were not associated with extreme river flooding or heavy rainfall and had mostly an easterly wave direction (roughly perpendicular to the coastline). Most importantly, evidence of runup was available for each. The model forcing for hindcasting historical storms was different than for the hazard assessment scenarios. A summary is given in Table 2-9 and a more in-depth description of each storm is provided below.

Table 2-9: Summary of runup from historical storms in Timaru District. Estimation of water level and wave conditions (Hs and Tp) are also provided. Wave angle of incidence is assumed to be normal to the offshore boundary of each model.

Storm date	Evidence	Water level (m LVD)	Hs (m)	Tp (s)
20-07-2001	Extensive coastal inundation; Milford hut seawall started overtopping; Debris 0.5 m below the stopbank at the end of Connolly Road.	1.6	5.9	13.5
03-04-2002	Milford Hut stopbank not overtopped but debris close-by; Pareora berm overwashed and inundation up to the rail tracks just north of meat works.	1.0	6.0	17.0
15-06-2012	Connolly Road runup to the top of stopbank. Aorangi road building gate with 0.3 m water depth.	0.9	6.0	16.0
15-08-2019	Debris on Connolly road stopbank and photos of overtopping.	1.0	5.5	18

2.6.1 20 July 2001 storm

The 2001 coastal inundation storm is used to verify the simulated runups and inundation extents and test the model sensitivity. The inundation extent digitized by Cope and Young (2001) was used to verify the overall methodology (Figure 2-7).

Storm conditions

Timaru Port tide gauge was not operational during the 2001 storm so water level was estimated to 1.6 m (LVD 47) based on Sumner tide gauge following Cope and Young (2001). ERA 5 global wave hindcast (C3S 2017) hints that waves recorded at the Steep Head wave buoy (Hs = 4.9 m) may have been lower than wave height on the Timaru coast (located much closer to the wave height peak). Wave conditions used for the simulation are based on the ERA 5 hindcast Hs = 5.9 m, Tp = 13.5 s. Waves are assumed to have fully refracted on the continental shelf and the wave crest reaches the shore nearly parallel to the coast.

Runup evidence

During the storm, sandbags were placed on the Milford Hut stopbank to prevent overtopping (Figure 2-3). This indicates that the water level may have reached near the top of the stopbank. Lidar data suggested a 4.2 m LVD elevation. At the stopbank located at the end of Connolly road (south of Opihi River) debris suggested the run up reached 0.5m below the stopbank (~5.7 to 5.8 m LVD).

Figure 2-3: Sandbags (white) placed on the Milford Hut stopbank during the 2001 Storm. Source: ECan.

2.6.2 04 April 2002 Storm

Waves and water level

Timaru Port tide gauge shows a clear signal of the storm waves peaking overnight on the 3rd of April 2002. Long waves reached above 1.2 m LVD but the still water level in the Port was more likely to be 1.0 m LVD. The Steep Head wave buoy recorded a wave height of 6 m at the same time with a peak period of 17 s and a wave direction of 120°.

Runup evidence

This storm brought long period waves that overtopped the beach just north of the Pareora meatworks factory and flooded the backshore there (Figure 2-4). Debris visible on Figure 2-4 suggests the runup reached around 5.5 m LVD close to the shore. This inundation extent is compared with the modelled inundation in Figure 2-7 and Figure 2-8.

Figure 2-4: Coastal inundation north of Pareora following the 2002 storm. Source: ECan.

2.6.3 15 June 2012 storm

Waves and water level

Timaru Port tide gauge shows a clear long wave signal on the 15 June 2012 at around mid-day. Long wave reached above 1.2m LVD but the still water level in the Port was more likely to be 0.9 m LVD. The Steep Head wave buoy recorded, at the same time, wave heights of 6.0 m with a peak period of 16 s and a wave direction of 150°.

Runup evidence

Debris was left by this storm on top of the coastal storm bank just south of Connolly road (South of Opihi River) (Figure 2-5). Debris and flattened grass also suggest the stopbank was overtopped in places. This suggests the runup reached at least 5.8 m LVD.

Near the sandblaster building at the end of Aorangi Road the inundation left debris on a fence gate indicating the flow depth reached 0.2 to 0.4 m which corresponds to a level of 2.9 to 3.1m LVD.

Figure 2-5: Debris left on stopbank south of Connolly road following June 2012 storm. Source: ECan.

2.6.4 15 August 2019 storm

Waves and water level

Timaru Port tide gauge shows a clear long wave signal on the 15 August 2019 at around mid-day. The long wave signal is also clear on the Opihi Lagoon water level recorder and in the Washdyke Lagoon water level recorder. In Timaru Port, the long wave reaches just above 1.2 m LVD. The still water level in the Port was more likely to be 1.0 m LVD. The Steep Head wave buoy recorded a wave height of 5.5 m at the same time, with a peak period of 18 s and a wave direction of 150°.

Runup evidence

ECan staff documented waves overtopping the seawall North of Connolly Road during this event. Debris left on top of the stopbank suggests a runup of 5.6m LVD.

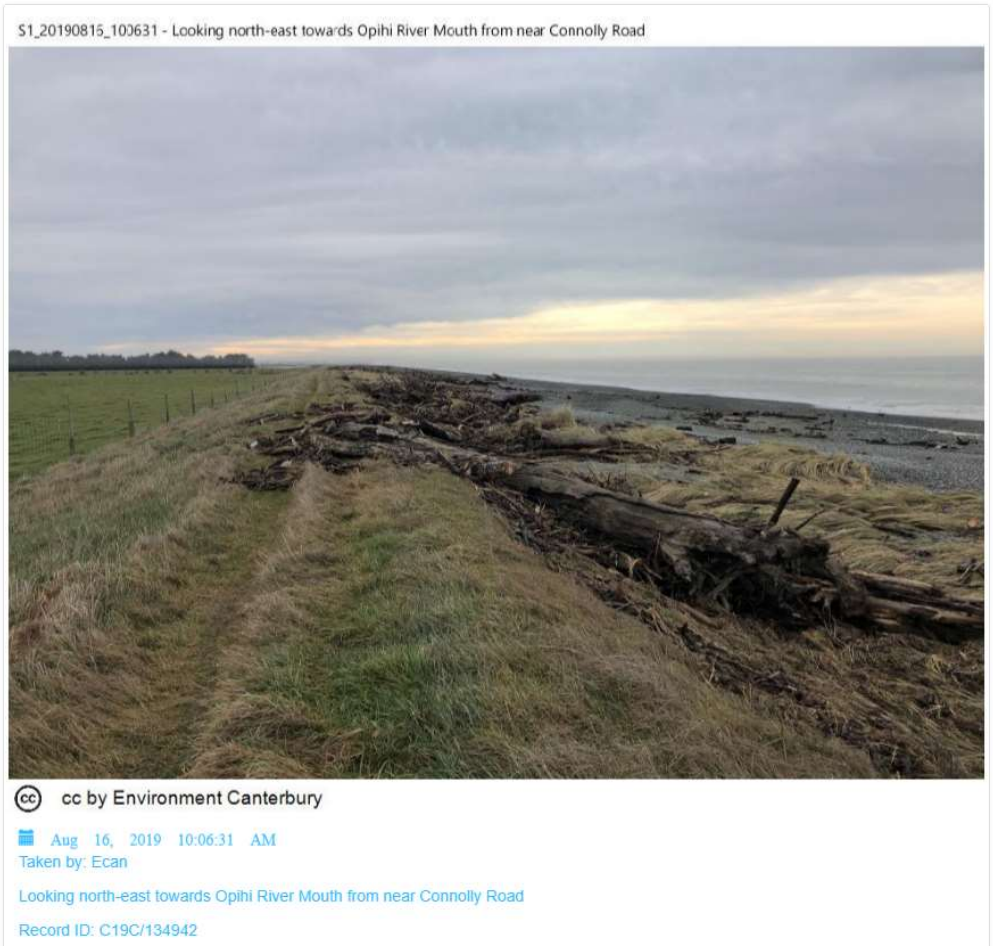

Figure 2-6: Debris left on stopbank north of Connolly road. Source: ECan.

2.6.5 Model validation

Breaker Index of 0.75 gives the most consistent inundation extent when comparing the model and recorded inundation for the 2001 storms (Figure 2-7). Using this breaker index values to simulate other storms also produces runups and inundation extent consistent with observation (Table 2-10 and Figure 2-8). However, the simulated runup are somewhat lower than observed. This is expected because the simulation does not account for the impact of beach erosion and overwashing (wave action lowering the beach berm) in this study. There is also a large uncertainty regarding the actual wave conditions during these events.

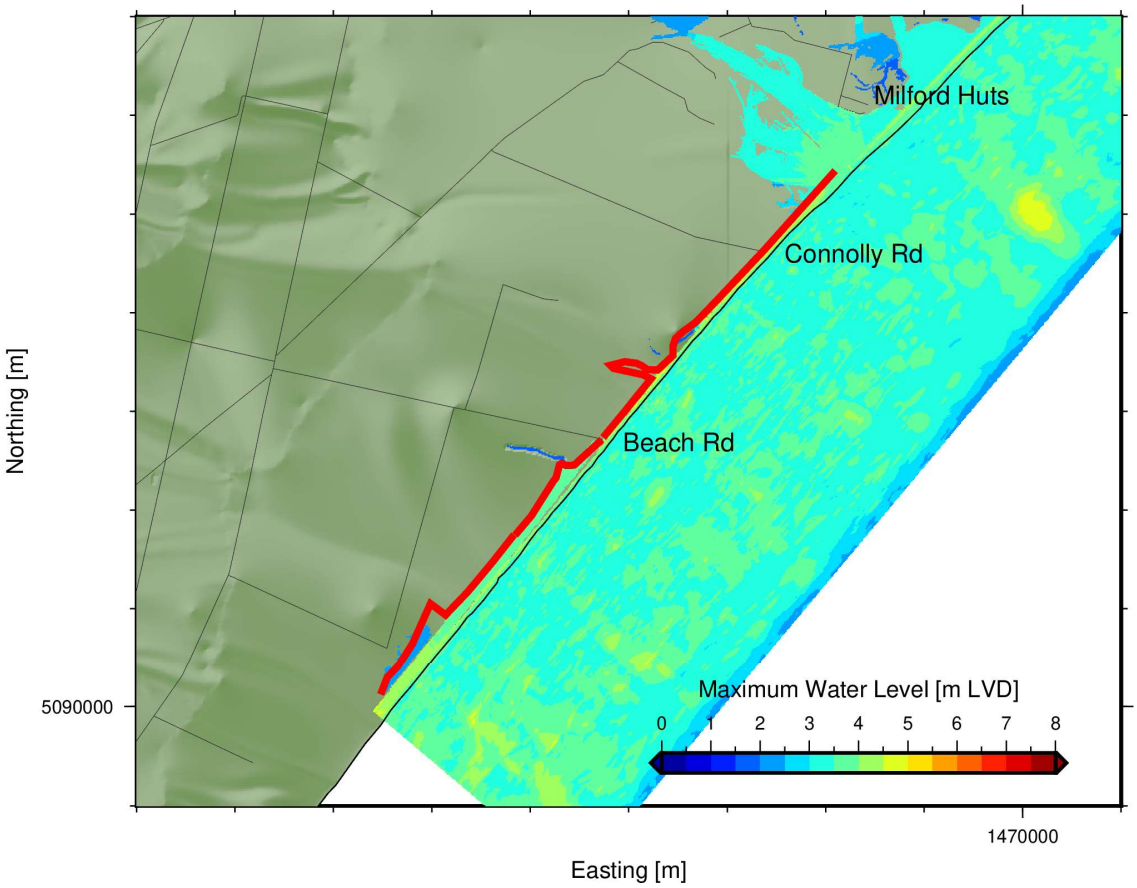

Figure 2-7: 2001 storm inundation simulated for Opihi. The red line shows the surveyed inundation extent by Cope & Young 2001. Also note that the inundation does not overtop the stop bank near Milford Huts.

Table 2-10: Comparison of observed run-up and simulated run-up for four storm events.

Storm	Location	Observed runup (m LVD)	Simulated runup (m LVD)
20-07-2001	Milford Hut	4.2	3.8
	Connolly Road	5.7	5.0
04-04-2002	Pareora	5.5	5.8
15-06-2012	Connolly Road	5.8	4.5
	Aorangi Road	3.1	2.6
15-08-2019	Connolly Road	5.6	5.3

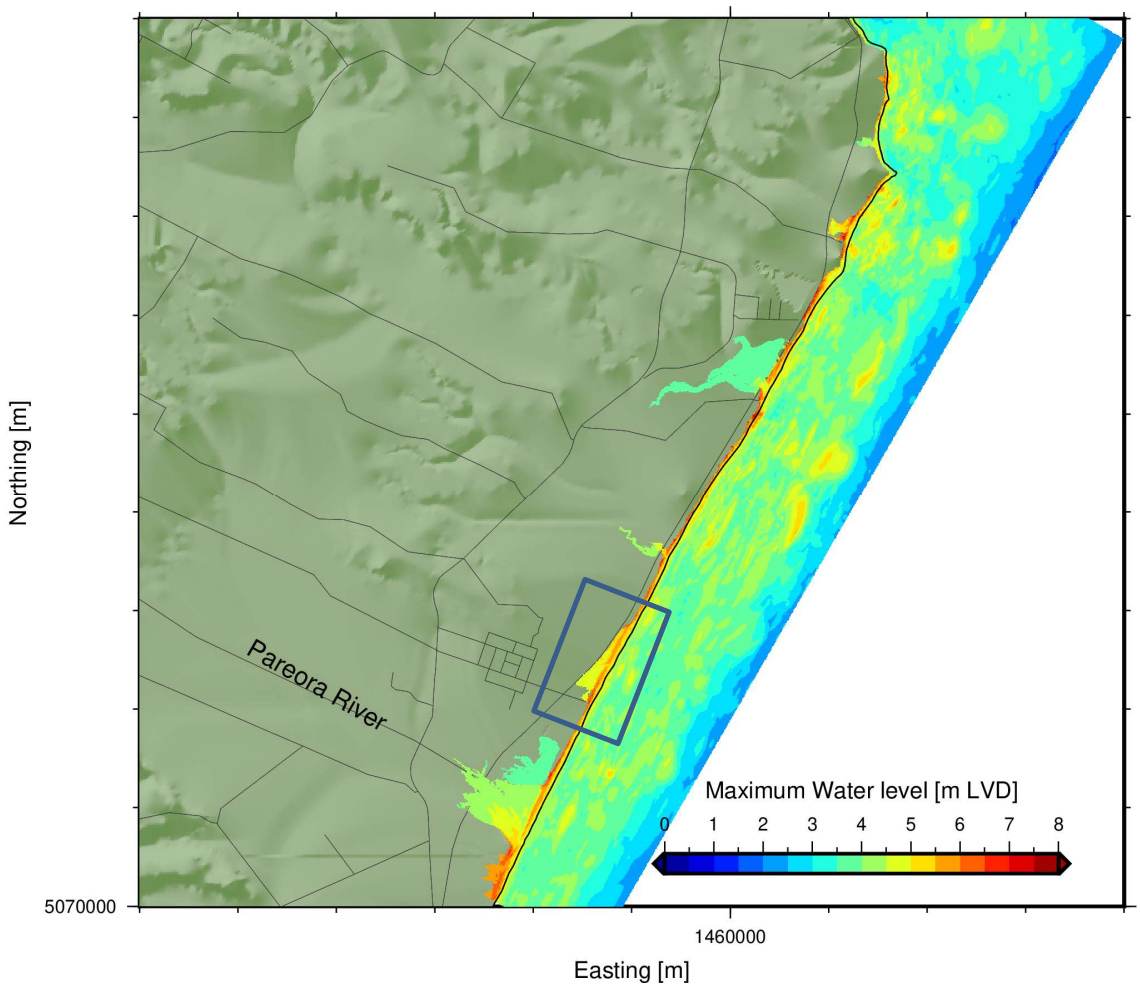

Figure 2-8: 2002 storm inundation simulated for Pareora to Saltwater Creek. Note the area in the box shows the inundation extent North of the Pareora River similar to the inundation extent shown in Figure 2-4; the shoreline in shown in thin black line and roads in thin grey lines.

3 Results

This study produced inundation overlay maps of maximum flow depth (i.e., maximum water level above ground) and maximum water level (i.e., above LVD datum) for nine scenarios of storm ARIs and SLR conditions. This section shows summaries of the coastal inundation from a 1% AEP storm under three sea level scenarios; present day sea-level, 0.8 m SLR and 1.5 m SLR (Figure 3-1, Figure 3-2, Figure 3-3 and Figure 3-4). For other scenarios, or details on water level or flow depth, refer to the accompanying GIS layers.

The 1% AEP storm for present mean sea level produces significant inundation throughout the district. The worst affected areas are the low-lying coastal plains north of Timaru, in particular, the area between the Opihi and the Orari Rivers where the inundation extent could reach 1km inland. A similar extent could affect low lying area bordering the Rangitata River and Pareora River. Waves during the 1% AEP storm are expected to overtop the Port Facility.

The simulation of a 1% AEP storm at present-day mean sea level shows that the exposed side (East side) of the Port is only flooded from the ocean side, mostly by large infragravity waves overtopping the seawall. The west arm of the Harbour gets affected by large infragravity waves in Caroline Bay that occasionally run up and over the boat ramps of the port facility (these appear to be initially formed from reflected waves on the south side of Dashing Rocks). The volume of water overtopping the structure is likely overestimated in the model because the damping effect of the rock revetment protecting the harbour is not taken into account in the model.

Incremental SLR scenarios show the areas inundated by storms increase. Coastal defences become less and less effective with higher water levels associated with sea level rise. Inundation extent due to the 1% AEP coastal storm nearly doubles from present to 0.8 m SLR and increases 2.5 times for 1.5 m SLR (Table 3-1) reaching 2.3 km inland just north of the Opihi River. In South Timaru, inundation could extend beyond the area covered by LiDAR survey. In the model the topography in these areas is based on the less certain DEM derived from topomap data.

Table 3-1: Total inundated area for all scenarios [km^2].

ARI\SLR	0.0	0.2	0.4	0.6	0.8	1.2	1.5
1% AEP	16.13	19.30	23.10	27.00	30.42	37.02	40.31
2% AEP			17.11	20.79			

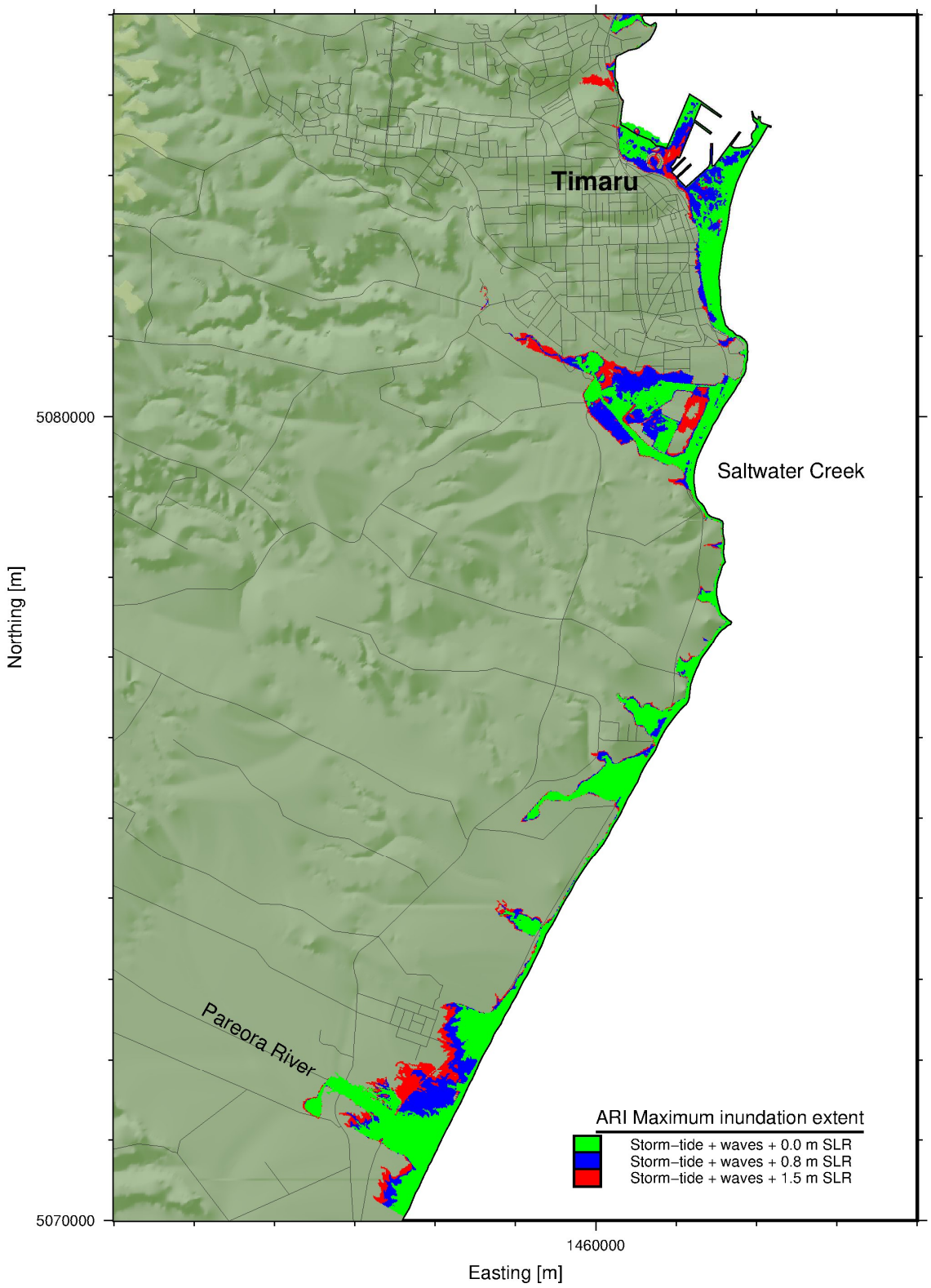

Figure 3-1: 1% AEP coastal inundation South of Timaru for present sea-level, 0.8 m SLR and 1.5 m SLR.

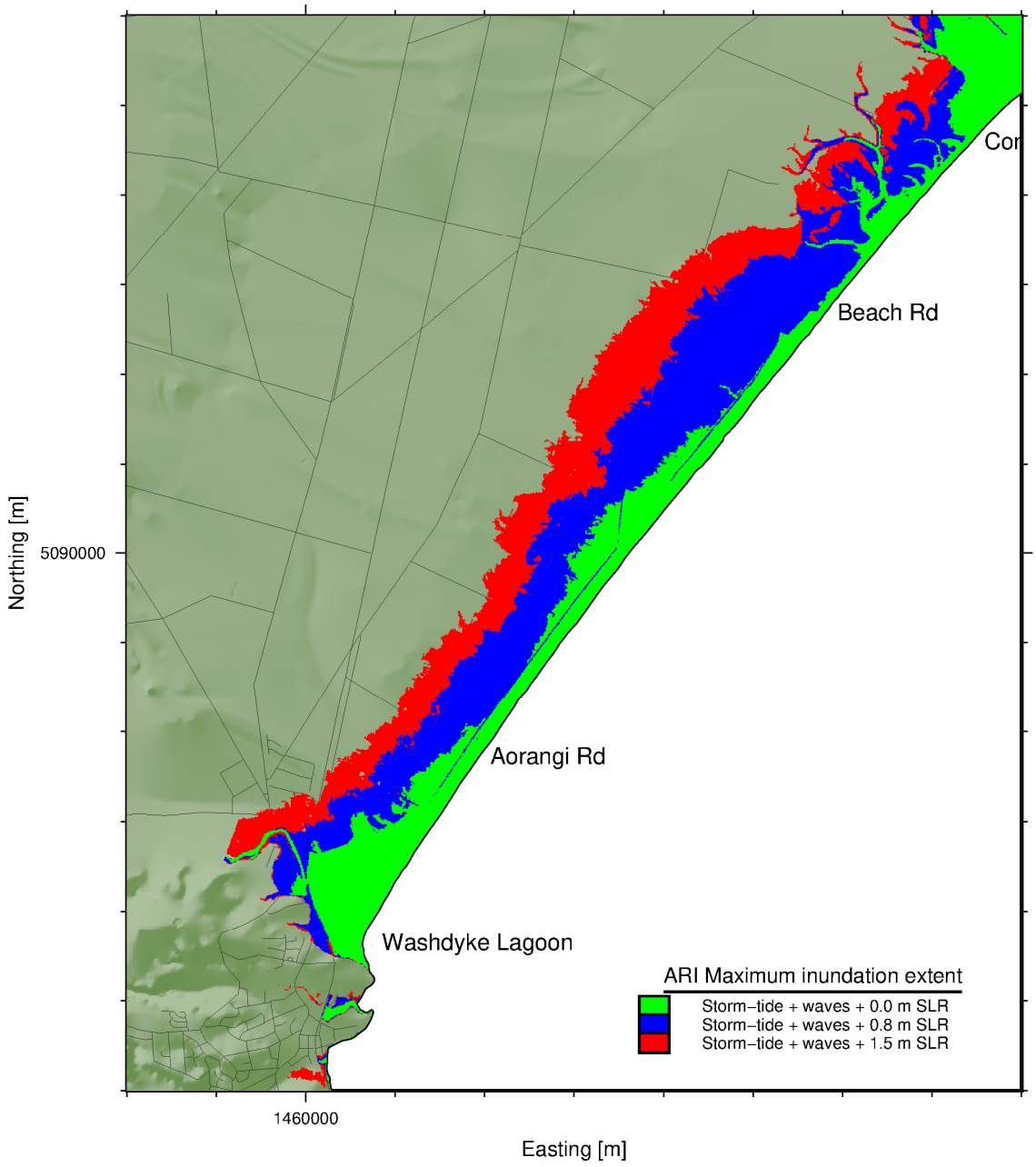

Figure 3-2: 1% AEP coastal inundation north of Timaru for present sea-level, 0.8 m SLR and 1.5 m SLR.

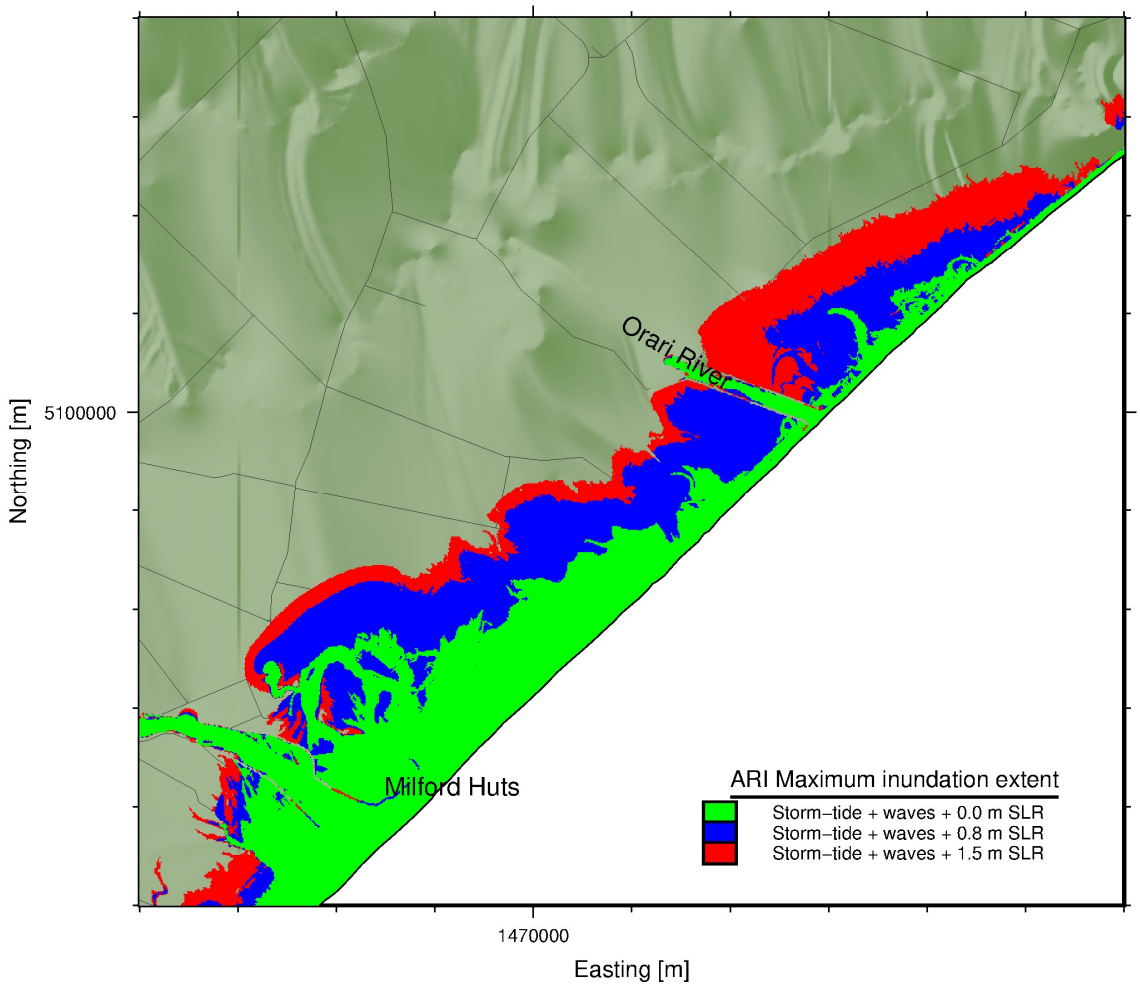

Figure 3-3: 1% AEP coastal inundation near Orari and Opihi rivers for present sea-level, 0.8 m SLR and 1.5 m SLR.

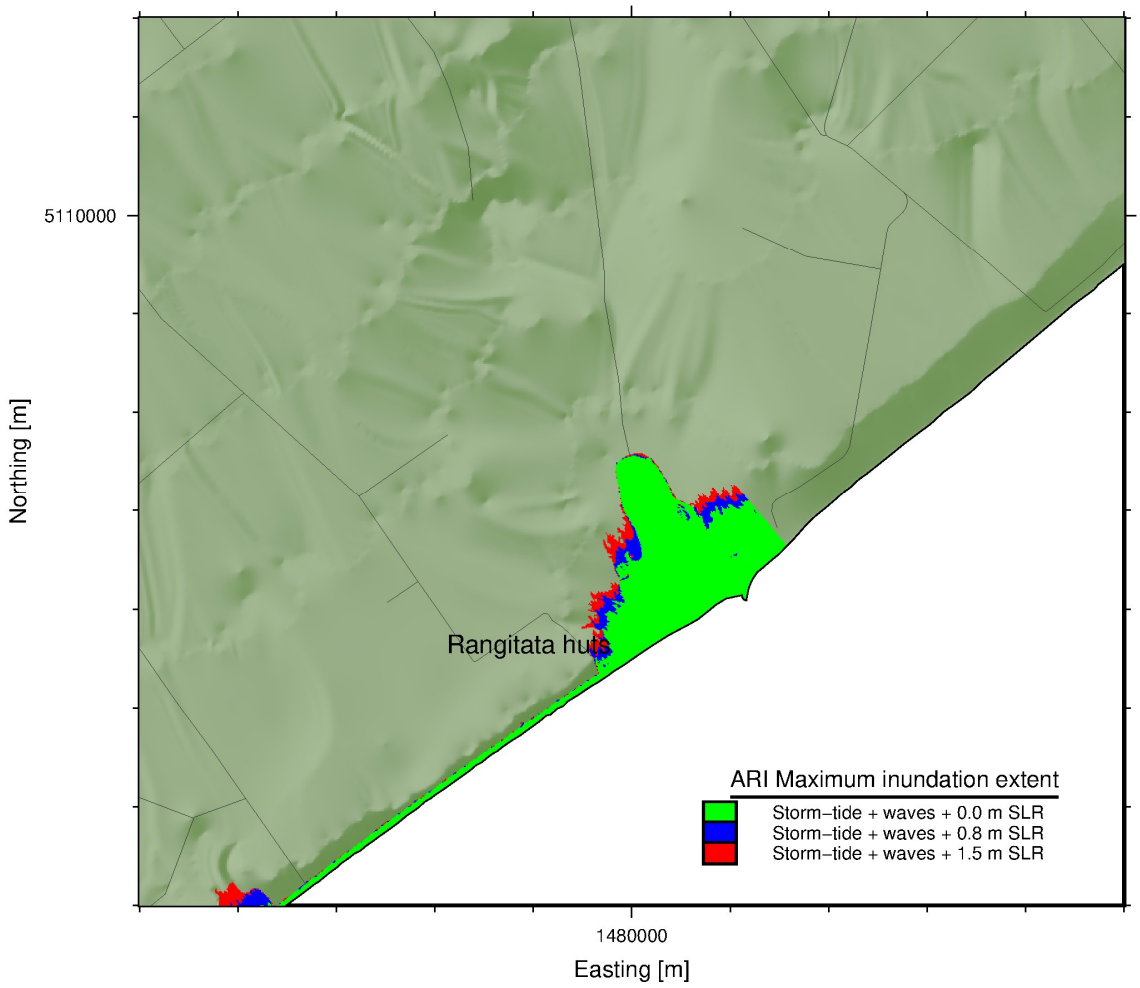

Figure 3-4: 1% AEP coastal inundation near Rangitata River for present sea-level, 0.8 m SLR and 1.5 m SLR.

4 Discussion

This study produces coastal inundation maps for 9 scenarios using a numerical model that simulates the main processes driving coastal inundation. The map produced are can be useful for planning and climate change adaptation but limitation inherent to the scenarios and the methodology need to be considered. These are discussed in detail below.

4.1 Stop-banks

Stop-banks are present along most of the coastline north of Timaru (red line in Figure 1-1). Some of the stop-banks are the result of recent flood management but others are older banks which have been partially lost to coastal erosion and/or have been damaged in previous storms. In the scenario considered in this study, the existing stop-banks (identified in Figure 1-1) are static. This implies that these stop-banks will be maintained to their present elevation (and position) in the future. The stop-bank enhancement technique used to guarantee stop-banks elevation in the model grid also overrules any flaw or weakening (lowering) in existing structures implying that the maintenance of stop-banks is current.

Most of the stop-banks present along the coast, although overtopped in large coastal storms, are effective at limiting the inundation extent. However, many of these structures are close to the present shoreline and threatened by coastal erosion. Therefore, the impact of coastal erosion and or damages to the stop-banks from storms could be considered as a signal in a climate change adaptation planning strategy to evaluate whether adaptation pathways are on-track or whether a switch to another adaptation pathway is required.

4.2 Role of river flooding in Rangitata and Milford/Opihi

In the simulations, mean annual maximum flow was used to produce a realistic flow in the river to account for the combined effect of coastal and river inundation. Using a mean annual annual flow only produces a first order assessment without consideration of the probability of co-occurrence/coincidence of large river flood peak with coastal storm peak. In all the 1% ARI ocean storm-tide simulations the coastal stop-bank and gravel barrier are overtopped producing inundation in the backshore eventually reaching the hut settlements at Rangitata and Opihi. The inclusion of river flow only exacerbates the inundation but the degree of exacerbation was not evaluated.

4.3 Limitation and caveats

Inherent uncertainties associated with the inundation modelling stem from the accuracy of the bathymetry, the resolution of the grid used, the model forcing, the numerical equations, the solver used for the modelling and whether the relevant processes are resolved. These uncertainties are described in more detail below.

The quality of the topographic data and the bathymetric data for inshore waters strongly influences the simulation of inundation. For this modelling, we used available LiDAR and DEM data for the land topography and navigation chart data, and coastal surveys for nearshore bathymetry. The bathymetry data is not as recent and is far coarser than the land topography and does not resolve small bathymetric features and morphological features that may be present (e.g., underwater outcrops, sand-banks). In addition, beach morphology changes rapidly during storms. The impact of beach erosion and overwashing (wave action lowering the beach berm) during storms is not taken into account in this study, but they are likely to influence the inundation depth and extent.

The study simulates inundation from coastal storms with future sea-level scenarios. In these scenarios the topography and bathymetry were not adjusted. However, it is likely that the morphology of beach profiles and gravel ridges will naturally adjust to sea-level rise (by retreating and/or rising). This long-term morphological adjustment of coastal geomorphologies as well as upgrades to stop-banks is not taken into account in this study.

Model uncertainty can be quantified by running multiple simulations with small variations in key parameters, an approach known as ensemble prediction or sensitivity analysis. Such an approach provides an envelope of predicted solutions, rather than single "scenario-type" predictions. However, running many simulations increases the computational costs, and, in any event, running ensembles would not quantify all of the uncertainties because our knowledge of all the processes involved in surf-zone dynamics and inundation remains incomplete.

The inundation modelling is based on storm-tide – wave joint probability of 1% AEP. This probability reflects the likelihood of the conditions offshore but not the likelihood of the inundation depths simulated here. In addition, there are uncertainties in the choice of ARI scenarios considered, here a conservative value of offshore significant wave height has been selected (95^{th} percentile confidence rather than maximum likelihood). This in turn produces a conservative assessment of the inundation that does not require the addition of a safety factor or freeboard.

The verification simulations in this study's is consistent with inundation and runup observations from selected historical storms with some bias (underestimation) in the model results. However, the scenarios were forced using the upper bound (95^{th} percentile confidence) of significant wave height for each recurrence interval which is conservative compared with forcing with maximum likelihood significant wave height. The overall conservative approach therefore removes the need for including any additional safety factor (i.e., freeboard) to the presented inundation layers.

4.4 Comparison with existing Sea Water Inundation Boundary

ECan produced a Sea Water Inundation Boundary to be included in the Regional Coastal Environment Plan (RCEP) and the Canterbury Regional Policy Statement (RPS). The boundary was created using information from historical events. The boundary is generally consistent with the modelled 1% AEP extent (Figure 4-1). However, the Sea Water Inundation Boundary extends further in-land between Beach Road and Phar Lap Road than the simulation result. The sea Water Inundation Boundary was constructed from inundation extent from historical storms. The boundary therefore includes area of compound flooding (e.g., rain and seawater combined) and inundation in storms that predate the construction of stop-banks.

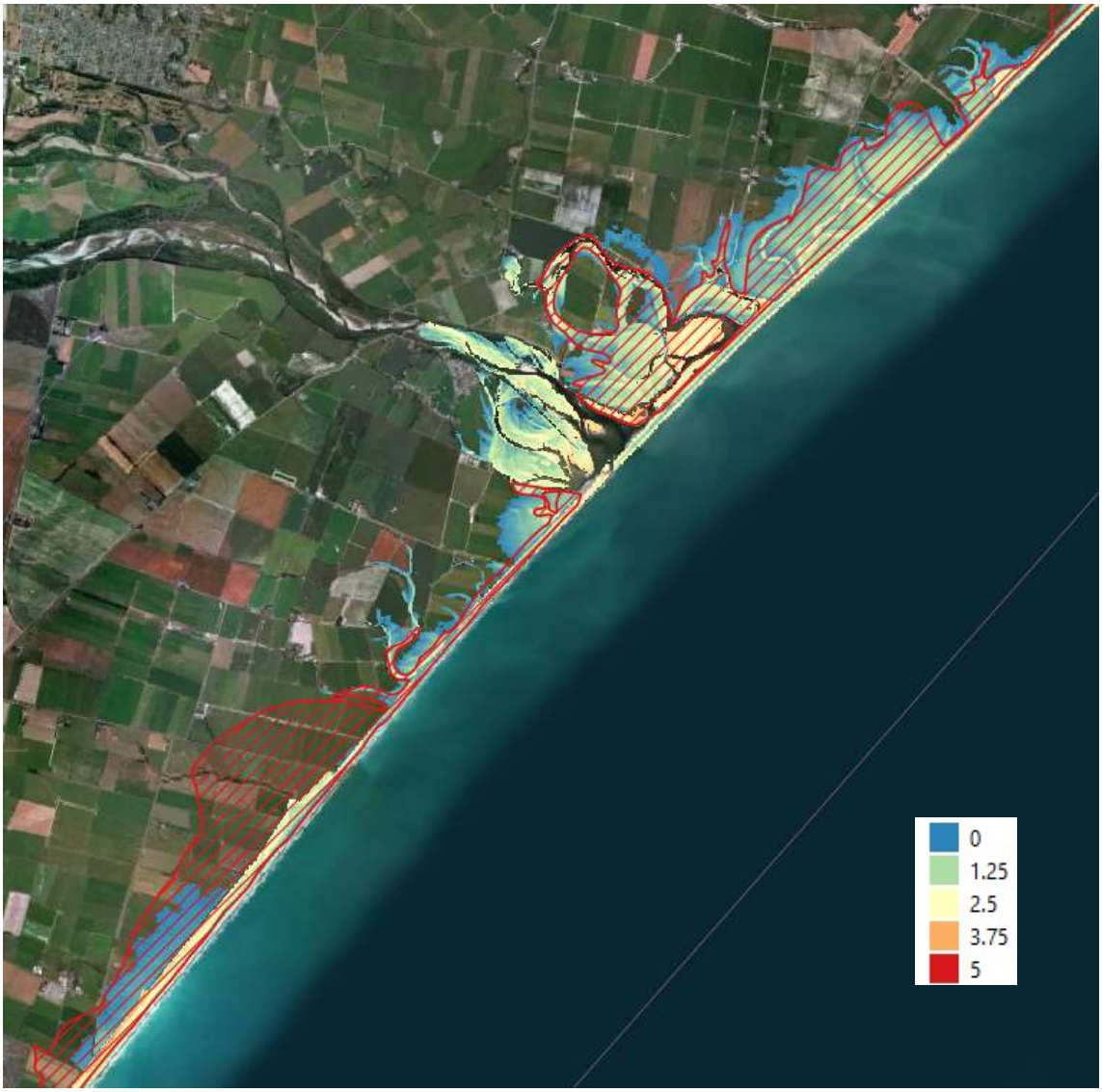

Figure 4-1: Comparison between ECAN Sea Water inundation boundary and this study's modelled flow-depth from the 1% AEP coastal storm at present mean sea level Near the Opihi River. the Sea Water inundation boundary is shown in red hachures and simulated flow depth [m] is shown in colour shading.

4.5 Comment on the sensitivity to breaker index (gamma) parameter

Using the 2001 storm conditions, a calibration was performed to identify the best wave dissipation parameter (i.e., Breaker index or gamma = 0.75 used in simulation above). Surf-zone hydrodynamics and runup strongly depends on how quickly waves dissipate when they break. Therefore, the simulated runup shows a high sensitivity to the wave dissipation terms. Wave dissipation in XBeach follows the Roelvink (1993) formulation suitable for group varying waves, with a default beaker index of 0.6. In the Canterbury bight the nearshore seafloor has a very mild slope and is relatively shallow causing large waves to start breaking relatively far offshore. These conditions (i.e., near flat seabed all the way to the shore) are significantly different from the conditions used to identify the default sets of XBeach parameters (dynamic barred beach and steep coarse sand beach) and may explain why a gamma value of 0.75 leads to better results. Unfortunately, only a thorough surf-zone

dynamics field investigation could confirm that this is the case. Other wave dissipation formulations (e.g., Daly et al. 2012) may be more suitable in the South Canterbury environment but there is not enough information available to justify using an alternative formulation, so the default formulation and calibrated gamma (0.75) were used here.

5 Conclusion

This study produced coastal inundation maps for the Timaru district between the Rangitata River in the North and the Pareora River in the South for seven scenarios of the 1% AEP storm at present mean sea level and for sea-level increments up to 1.5 m as well as two scenarios of SLR for the 2% AEP storm. GIS layers accompanying the document show the details of flow depth, maximum water-level and inundation extent. The 1% AEP simulation at present-day mean sea level produces significant inundation throughout the district generally consistent with the existing Sea Water Inundation Boundary (ECAN). The inundated area for the same ARI doubles with 0.8 m SLR and for 1.5m SLR the area increases 2.5 times.

Between Washdyke Lagoon and the Rangitata River, stop-banks present along the coast, although overtopped during large coastal storms, are effective at limiting the inundation extent but the effect of these structures diminishes with SLR. The role of stop-bank is important in monitoring and planning for climate change adaption pathways. In South Timaru, the inundation extent can exceed the area covered by LiDAR topography for SLR of 1.5 m leading to uncertainty in the results there.

The study has limitations inherent to the scenarios and the methodology. Simulations of historical storms showed consistent results when compared to observations, with a potential underestimation. However, the overall approach is conservative and should not require the inclusion any additional safety factor (i.e., freeboard) to the presented inundation layers.

6 Acknowledgements

Most of the figures in this report as well as some data pre-processing and model output post-processing was completed using the Generic Mapping Tool Package (Wessel et al. 2013).

7 References

Ali, M. (2001) Potential runoff Accumulation in the Wheatbelt towns of Western Australia. Department of Agriculture and Food, Western Australia, Perth. *Report,* 226.

Arcement, G.J., Schneider, V.R. (1989) Guide for selecting Manning's roughness coefficients for natural channels and flood plains. *USGS Water Supply Paper,* 2339.

Bosserelle, C. (2013) *Morphodynamics and sand transport on perched beaches*. PhD Thesis. University of Western Australia, Crawley, Australia.

Chow, V.T. (1959) *Open-channel hydraulics*. New York, McGraw-Hill Book Co.

Columbus, J. (2011) *An assessment of fractal interpolation for deriving Digital Elevation Models (DEM)*, Honours thesis, School of Surveying, University of Otago.

Copernicus Climate Change Service (C3S) (2017) ERA5: Fifth generation of ECMWF atmospheric reanalyses of the global climate. Copernicus Climate Change Service Climate Data Store (CDS), https://cds.climate.copernicus.eu/cdsapp#!/home

Daly, C., Roelvink, D., van Dongeren, A., van Thiel de Vries, J., McCall, R., (2012) Validation of an advective-deterministic approach to short wave breaking in a surf-beat model. *Coastal Engineering*, 60(69-83): 0378-3839. https://doi.org/10.1016/j.coastaleng.2011.08.001.

Deltares (2019) *XBeach skillbed report*, revision 5571, status update trunk default, May 2019. Available at https://content.oss.deltares.nl/xbeach/testbed/report/trunk_default_2019057.pdf

DoC (2010) *New Zealand Coastal Policy Statement 2010*. Department of Conservation: 38.

Engman, E.T. (1986) Roughness Coefficients for Routing Surface Runoff. *Journal of Irrigation and Drainage Engineering,* 112: 39-53.

Henderson, F.M. (1966) *Open channel flow*. New York, Macmillan.

MfE (2017) Coastal hazards and climate change: Guidance for local government. *Ministry for the Environment Publication* ME1341. Wellington, Ministry for the Environment: 279 p. + Appendices http://www.mfe.govt.nz/publications/climate-change/coastal-hazards-and-climate-change-guidance-local-government. Wellington, Ministry for the Environment.

Musleh, F.A., Cruise, J.F. (2006) Functional Relationships of Resistance in Wide Flood Plains with Rigid Unsubmerged Vegetation. *Journal of Hydraulic Engineering,* 132: 163-171.

Narayan, S. et al. (2017) The Value of Coastal Wetlands for Flood Damage Reduction in the Northeastern USA. *Scientific Reports,* 7: 9463.

Roelvink, D., Reniers, A., van Dongeren, A., de Vries, J.V., McCall, R., Lescinski, J. (2009) Modelling storm impacts on beaches, dunes and barrier islands. *Coastal Engineering,* 56: 1133-1152.

Roelvink, J.A. (1993) Dissipation in random wave group incident on a beach. *Coastal Engineering*, 19: 127–150.

Smith, W.H.F, Wessel, P. (1990) Gridding with continuous curvature splines in tension. *Geophysics*, 55: 293-305.

Stephens, S.A., Allis, M., Robinson, B., Gorman, R.M. (2015) Storm-tides and wave runup in the Canterbury Region. Prepared for Environment Canterbury. *NIWA Client Report* HAM2015-129: 133.

Townsend, M., Wadhwa, S. (2017) Developing automated methods for mapping estuarine vegetation. *National institute of Water and Atmospheric Research Ltd.*

Wessel, P., Smith, W.H.F., Scharroo, R., Luis, J., Wobbe F. (2013) Generic Mapping Tools: Improved Version Released. *EOS Trans. AGU*, 94(45): 409-410. doi:10.1002/2013EO450001.

Zhang, K., Liu, H., Li, Y., Xu, H., Shen, J., Rhome, J., Smith, T.J. (2012) The role of mangroves in attenuating storm surges. *Estuarine, Coastal and Shelf Science,* 102-103: 11-23.